

# Comprehensive analysis of autophagy- and glycolysis-related differentially expressed genes involved in chronic inflammation in obese patients.

Simin Yang<sup>1</sup>, Rexidanmu Hudabai<sup>1</sup> and Xinwei Su<sup>2</sup>

<sup>1</sup>Department of Anesthesiology, The Fifth Affiliated Hospital of Sun Yat-sen University, Zhuhai, Guangdong, China.

<sup>2</sup>Department of Obstetrics and Gynecology, The Fifth Affiliated Hospital of Sun Yat-sen University, Zhuhai, Guangdong, China.

**Keywords:** Obesity; Autophagy; Glycolysis; Inflammation.

**Abstract.** The interaction between glycolysis and autophagy contributes to reprogramming chronic inflammation in obesity, but the knowledge about this interaction remains limited. Publicly available data were used to analyze autophagy- and glycolysis-related differentially expressed genes (A&GRDEGs) in two datasets comparing patients with obesity and normal-weight patients. A total of 5 A&GRDEGs were obtained through screening, namely recombinant eukaryotic translation initiation factor 4E binding protein 1 (*EIF4EBP1*), transforming growth factor beta 1 (*TGFBI*), fatty acid synthase (*FASN*), alpha-synuclein (*SNCA*), and C-X-C chemokine receptor 4 (*CXCR4*). Levels of autophagy and glycolysis exhibit substantial predictive value for obesity development and mechanistically contribute to disease pathogenesis through immunometabolic dysregulation.

## **Análisis exhaustivo de los genes expresados diferencialmente, relacionados con la autofagia y la glucólisis, que intervienen en la inflamación crónica en pacientes obesos.**

*Invest Clin* 2025; 66 (4): 390 – 407

**Palabras clave:** Obesidad; Autofagia; Glucólisis; Inflamación.

**Resumen.** La interacción entre la glucólisis y la autofagia contribuye a la reprogramación de la inflamación crónica en la obesidad, pero el conocimiento sobre esta interacción es limitado. Se utilizaron datos públicamente disponibles para analizar los genes expresados diferencialmente relacionados con la autofagia y la glucólisis (A&GRDEG) entre pacientes con obesidad y con peso normal en dos conjuntos de datos. Se obtuvo un total de 5 A&GRDEG mediante cribado, a saber: la proteína recombinante de unión al factor de iniciación de la traducción eucariótica 4E 1 (EIF4EBP1), el factor de crecimiento transformante beta 1 (TGFB1), la sintasa de ácidos grasos (FASN), la alfa-sinucleína (SNCA) y el receptor de quimiocina C-X-C 4 (CXCR4). Los niveles de autofagia y de glucólisis mostraron un valor predictivo elevado para el desarrollo de la obesidad y contribuyen mecánicamente a la patogénesis de la enfermedad mediante la desregulación inmunometabólica.

*Received:* 03-08-2025    *Accepted:* 21-09-2025

### **INTRODUCTION**

According to projections, the global population of people living with obesity, a metabolic syndrome, will reach one billion by 2030, affecting one in five women and one in seven men <sup>1</sup>. Obesity is characterized by excess weight (body mass index, BMI  $\geq 30$  kg/m<sup>2</sup>), accompanied by chronic low-grade inflammation, oxidative stress, insulin resistance, hypertension, dyslipidemia, and other abnormalities. It could also increase the susceptibility of individuals to chronic diseases, such as type 2 diabetes mellitus (T2DM), non-alcoholic fatty liver disease (NAFLD), and specific malignancies <sup>2</sup>. Furthermore, adipocytes serve as central metabolic and inflammatory regulators through their endocrine capacity, secreting both pro- and anti-inflammatory mediators, including leptin (pro-inflammatory) and adiponectin (anti-

inflammatory), which systemically influence energy homeostasis and immune responses<sup>1</sup>. Leptin and adiponectin exert pro-inflammatory and anti-inflammatory functions, respectively, and mutually regulate carcinogenesis <sup>2</sup>.

Adequate lipid storage prevents ectopic lipid accumulation in non-specific organs (e.g. muscle, liver, and heart) and toxic lipid accumulation (e.g., lipotoxicity) and is also associated with stable metabolic function <sup>3</sup>. Lipid droplet accumulation in the liver and other organs has been linked with obesity-associated autophagic dysfunction <sup>4</sup>. The seminal recognition of autophagy through the 2016 Nobel Prize in Physiology or Medicine underscores its pivotal role as a fundamental cellular clearance mechanism for superfluous or deleterious constituents<sup>5</sup>. Chronic inflammation in individuals with obesity may suppress autophagy. Moreover,

obesity-associated autophagic dysfunction may cause protein and organelle degradation, cellular dysfunction, and cell death <sup>6</sup>. Autophagy is presumed to be inactive during obesity owing to the chronic upregulation of mammalian target of rapamycin complex 1 (mTORC1) <sup>7</sup>. Obesity could contribute to an elevated risk of cancer through autophagic impairment; thus, treatment methods involving the enhancement of autophagy may serve as a practical approach against obesity-associated cancers <sup>8</sup>.

Metabolism is widely known as a core process underpinning all biological phenomena, supplying energy and building blocks for macromolecules <sup>9</sup>. Restricting glycolysis has been shown to impede cytokine production but not cellular proliferation, suggesting that glycolysis plays a critical role in regulating inflammation <sup>10</sup>. However, information on the exact mechanism by which the interaction between glycolysis and autophagy contributes to reprogramming the progression of chronic inflammation in obesity remains limited.

Individuals with obesity exhibit adipocyte hypoxia, which could lead to the elevated expression of hypoxia-inducible factors, activation of adipocytes, production and release of free fatty acids and pro-inflammatory mediators, induction of circulating monocyte recruitment, and aggregation of adipose tissue macrophages <sup>11</sup>. Studies have revealed that individuals with obesity have a higher macrophage count in white adipose tissues than individuals with normal BMI, showing increases ranging from 10% to >50% of the total cell count <sup>12</sup>. Metabolically activated macrophages show a higher rate of glycolysis and produce more lactic acid in the fatty tissues of individuals with obesity than in the tissues of normal-weight individuals <sup>13</sup>. Alterations in immune cell infiltration dynamics and their secretion of pro-inflammatory cytokines critically contribute to the sustained low-grade inflammation observed in obesity. Consequently, targeting immune cell recruitment and activation has emerged as a

key therapeutic strategy for obesity-associated chronic inflammation <sup>14</sup>.

In this study, screening was first performed to identify genes frequently involved in autophagy and glycolysis. Next, we leveraged publicly available datasets to compare the expression profiles of autophagy- and glycolysis-related genes between obese and normal-weight individuals. Additionally, we assessed immune cell infiltration patterns and examined their correlations with the differentially expressed genes. These findings could help elucidate the key mechanisms underlying the pathogenesis of chronic inflammation in patients with obesity and provide potential targets for prevention and treatment.

## MATERIALS AND METHODS

### Dataset download and processing

We obtained two obesity-related gene expression datasets (GSE134913 <sup>15</sup> and GSE59034 <sup>16</sup>) from the Gene Expression Omnibus (GEO) database (<https://www.ncbi.nlm.nih.gov/geo/>). The GSE134913 dataset included samples. We included 14 pre-surgery samples from obese patients (Obese group) who underwent metabolic surgery and six controls (Control group), forming a subset of 20 samples.

The GSE134913 dataset is a subset of participants from the GSE135066 cohort. It comes from the clinical study “Dynamic Changes in Muscle Insulin Sensitivity after Metabolic Surgery” by Gancheva *et al.* <sup>15</sup>. The original cohort included six control subjects and 16 obese individuals who had metabolic surgery, with longitudinal gene expression profiling done at three timepoints: before surgery, two weeks after surgery, and 52 weeks after surgery. For this analysis, we included all six control subjects and 14 of the 16 obese participants who had surgery, based on data completeness criteria.

Although aggregate baseline characteristics of the entire cohort are provided in the original publication, detailed demographic and clinical metadata for the specific genet-

ic sequencing subset were unavailable. As a result, participant-level clinical information could not be included in our analyses.

The GSE59034 dataset contained 48 samples. We selected 16 pre-surgery obese samples and 16 controls, yielding a total of 32 samples. This dataset served as the primary cohort for all subsequent analyses. Detailed information about the datasets is provided in Table S1.

Autophagy-related genes (ARGs) and glycolysis-related genes (GRGs) were systematically identified through comprehensive searches of the GeneCards database (<https://www.genecards.org>), followed by literature validation using PubMed (<https://pubmed.ncbi.nlm.nih.gov/>) with “Autophagy”<sup>17-19</sup> and “Glycolysis”<sup>20-22</sup> as the primary search terms, respectively. The intersection of ARGs and GRGs defined the autophagy- and glycolysis-related genes (A&GRGs) used in this study (Fig. 1).

Differentially expressed genes analysis

Based on the original study designs, samples were stratified into control and obese groups. Differentially expressed genes (DEGs) were identified using the limma package (v3.58.1) in R (v4.2.2), with significance defined as  $|\log FC| > 0.5$  and  $p < 0.05$ . Results were visualized through volcano plots (ggplot2, v3.4.4).

To obtain the autophagy- and glycolysis-related differentially expressed genes (A&GRDEGs), we first intersected all significant DEGs with our curated list of A&GRGs, and a Venn diagram was plotted to provide the A&GRDEGs. Expression patterns of these A&GRDEGs were subsequently displayed as clustered heatmaps (pheatmap package, v1.0.12) in R, using z-score normalized expression values.

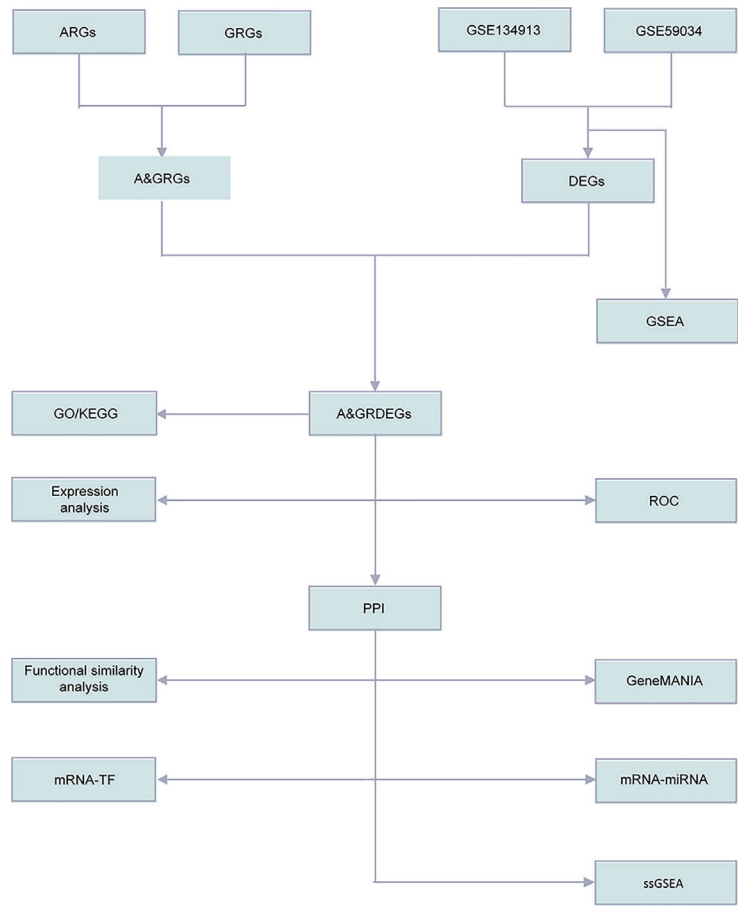


Fig. 1. Technology roadmap.

ARGs, Autophagy Related Genes. GRGs, Glycolysis Related Genes. A&GRGs, Autophagy & Glycolysis Related Genes. A&GRDEGs, Autophagy & Glycolysis Related Differentially Expressed Genes. DEGs, Differentially expressed genes. GSEA, Gene Set Enrichment Analysis. GO, Gene Ontology. KEGG, Kyoto Encyclopedia of Genes and Genomes. ssGSEA, single-sample gene-set enrichment Analysis. ROC, receiver operating characteristic curve. PPI, Protein-protein interaction network. TF, Transcription factors.

### Gene ontology and Kyoto Encyclopedia of Genes and Genomes pathway enrichment analyses

Functional enrichment analysis was performed using the clusterProfiler package (v4.10.0) in R. Gene Ontology (GO) and Kyoto Encyclopedia of Genes and Genomes (KEGG) pathway analyses were conducted on the differentially expressed genes. Terms with  $p < 0.05$  and false discovery rate (FDR;  $q$ )  $< 0.25$  were considered statistically significant.

### Gene Set Enrichment Analysis

Gene Set Enrichment Analysis (GSEA) was conducted on the GSE59034 dataset using the clusterProfiler package. Genes were ranked by  $\log_2$  fold-change and analyzed against the 'c2.all.v2022.1.Hs.symbols.gmt' gene set (All Canonical Pathways,  $n=3,050$ ) from MSigDB, with *Homo sapiens* as the reference species. Significance thresholds were set at  $p < 0.05$  and  $q < 0.25$ .

### Differential expression and receiver operating characteristic analyses of A&GRDEGs

The expression patterns of A&GRDEGs were compared between the obese and control groups across both datasets. The diagnostic potential was evaluated using receiver operating characteristic (ROC) analysis performed with the pROC package (v1.18.5). Area under the curve (AUC) values were determined to measure the predictive ability.

### Analysis of immune infiltration

Immune cell infiltration levels were quantified using single-sample Gene Set Enrichment Analysis (ssGSEA) implemented in the GSVA package (v1.50.0). Correlations among differentially abundant immune cell populations (obese vs. control), and between immune cells and A&GRDEG expression, were analyzed in the GSE59034 dataset. Results were visualized as correlation dot plots (ggplot2).

### Statistical analysis

All statistical analyses were conducted using R software (R Foundation for Statistical Computing, Vienna, Austria). Continuous variables were compared with Student's t-test (for normally distributed data) or Wilcoxon rank-sum test (for non-normal data). Multi-group comparisons employed the Kruskal-Wallis test. Categorical variables were analyzed with  $\chi^2$  tests or Fisher's exact tests, depending on the situation. Correlations were assessed with Spearman's rank correlation. A two-tailed  $\alpha$  level of 0.05 was deemed statistically significant unless otherwise noted.

## RESULTS

### Identification of A&GRDEGs

Differential expression analysis revealed 628 significant DEGs ( $|\log_{2}FC| > 0.5$  and  $p < 0.05$ ) in the GSE134913 dataset, comprising 316 upregulated and 312 downregulated genes (Fig. 2A). The GSE59034 dataset showed more pronounced differential expression with 904 DEGs under the same thresholds (653 upregulated, 251 downregulated; Fig. 2B). Volcano plots visually represent these expression patterns, highlighting the asymmetric distribution of upregulated versus downregulated genes between datasets.

To identify the A&GRDEGs, we intersected the significant DEGs ( $|\log_{2}FC| > 0.5$  and  $p < 0.05$ ) from both datasets with our curated A&GRG list, revealing five overlapping genes (Fig. 2C): eukaryotic translation initiation factor 4E binding protein 1 (*EIF4EBP1*), transforming growth factor beta 1 (*TGFB1*), fatty acid synthase (*FASN*), alpha-synuclein (*SNCA*), and C-X-C chemokine receptor type 4 (*CXCR4*) (Table 1). We subsequently analyzed and visualized the differential expression patterns of these A&GRDEGs between sample groups in the GSE134913 dataset (Fig. 2D) and in the GSE59034 dataset (Fig. 2E).



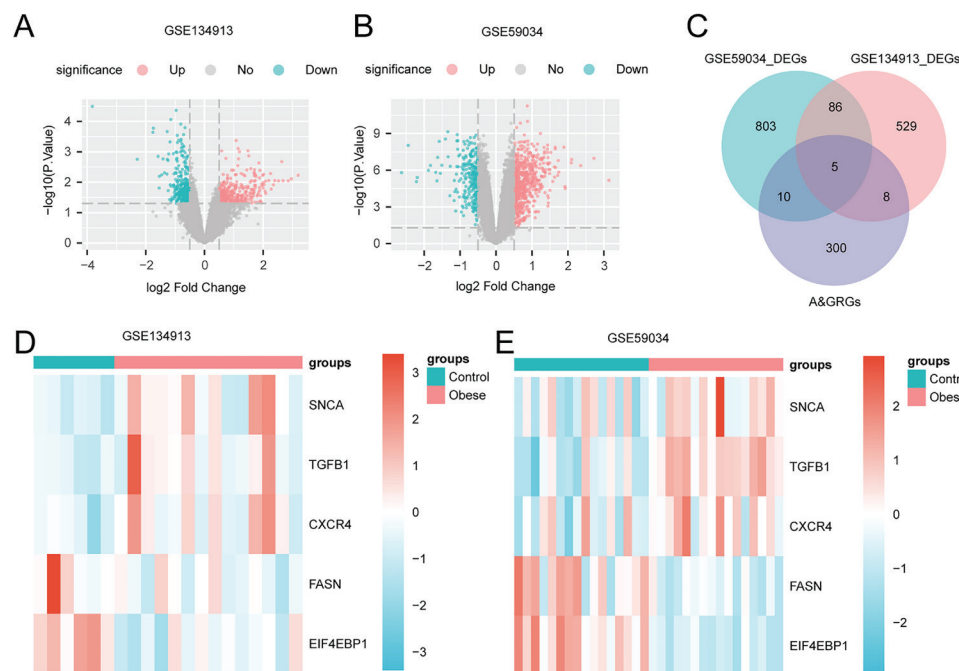


**Fig. 2.** Differentially expressed genes (DEGs) analysis. (A) Volcano plot of differential analysis results between the obese and control groups in the GSE134913 dataset. (B) Volcano plot of differential analysis results between the obese and control groups in the GSE59034 dataset. (C) Venn diagram of DEGs in the GSE134913 and GSE59034 datasets and A&GRGs. (D) Differential expression heatmap of DEGs in the GSE134913 dataset. (E) Differential expression heatmap of DEGs in the GSE59034 dataset. Green indicates the control group, and orange indicates the obese group. In the heatmaps, blue represents low expression, and red represents high expression.

**Table 1.** A&GRDEGs in GSE59034 and GSE134913.

	Gene	logFC	AveExpr	t	p	p adjust	B	group
GSE59034	EIF4EBP	-0.75697	6.168652	-7.58047	8.52E-09	3.51E-06	10.16121	down
	TGFB1	0.571166	6.797319	5.933876	1.06E-06	4.33E-05	5.525466	up
	FASN	-0.64127	10.46345	-4.02795	0.0003	0.002172	0.123576	down
	SNCA	0.596172	7.741707	2.504538	0.017237	0.049432	-3.63114	up
	CXCR4	0.512738	6.194027	2.197896	0.034888	0.085782	-4.25343	up
	EIF4EBP	-0.79216	9.560483	-4.21636	0.00039	0.901994	-3.5489	down
GSE134913	SNCA	1.325622	9.526431	2.616228	0.016162	0.999958	-4.10701	up
	CXCR4	0.785232	7.648631	2.278605	0.033299	0.999958	-4.22823	up
	TGFB1	1.137448	6.567356	2.192964	0.039755	0.999958	-4.25833	up
	FASN	-0.57511	7.727896	-2.11711	0.046404	0.999958	-4.28468	down

**Construction and analysis of the prediction model**

We systematically investigated the functional associations of the five A&GRDEGs with obesity through comprehensive GO and

KEGG enrichment analyses (Table 2). GO analysis identified significant enrichment in biological processes (BP) such as positive regulation of glial cell differentiation, receptor metabolic process, and gliogenesis; cellular

**Table 2.** Gene Ontology (GO) and Kyoto Encyclopedia of Genes and Genomes (KEGG) enrichment analysis results.

Ontology	ID	Description	Gene Ratio	Bg Ratio	p	p adjust	q	geneID	Count
BP	GO:0032103	positive regulation of response to external stimulus	3/5	442/18800	0.00012461	0.02430796	0.00669754	TGFB1/ SNCA/ CXCR4	3
BP	GO:0045687	positive regulation of glial cell differentiation	2/5	42/18800	4.8517E-05	0.02430796	0.00669754	TGFB1/ CXCR4	2
BP	GO:0043112	receptor metabolic process	2/5	61/18800	0.00010291	0.02430796	0.00669754	TGFB1/ SNCA	2
BP	GO:0014015	positive regulation of gliogenesis	2/5	64/18800	0.00011333	0.02430796	0.00669754	TGFB1/ CXCR4	2
BP	GO:2000379	positive regulation of reactive oxygen species metabolic process	2/5	71/18800	0.0001396	0.02430796	0.00669754	TGFB1/ SNCA	2
CC	GO:0031091	platelet alpha granule	2/5	91/19594	0.0002114	0.00718767	0.00400552	TGFB1/ SNCA	2
CC	GO:0031092	platelet alpha granule membrane	1/5	17/19594	0.00433098	0.07362671	0.04103037	SNCA	1
CC	GO:0031093	platelet alpha granule lumen	1/5	67/19594	0.01698227	0.08811426	0.04910392	TGFB1	1
CC	GO:0016234	inclusion body	1/5	74/19594	0.01874314	0.08811426	0.04910392	SNCA	1
CC	GO:0005902	microvillus	1/5	90/19594	0.0227585	0.08811426	0.04910392	TGFB1	1
MF	GO:0003779	actin binding	2/5	439/18410	0.00540893	0.04141684	0.01278836	SNCA/ CXCR4	2
MF	GO:0008190	eukaryotic initiation factor 4E binding	1/5	10/18410	0.00271326	0.04141684	0.01278836	EIF4EBP1	1
MF	GO:0034713	Type I transforming growth factor beta receptor binding	1/5	10/18410	0.00271326	0.04141684	0.01278836	TGFB1	1
MF	GO:0004312	fatty acid synthase activity	1/5	13/18410	0.00352609	0.04141684	0.01278836	FASN	1
MF	GO:0043027	cysteine-type endopeptidase inhibitor activity involved in the apoptotic process	1/5	22/18410	0.0059614	0.04141684	0.01278836	SNCA	1
KEGG	hsa04672	Intestinal immune network for IgA production	2/5	49/8164	0.00034888	0.02163052	0.01652586	TGFB1/ CXCR4	2
KEGG	hsa04152	AMPK signaling pathway	2/5	121/8164	0.00211594	0.05414617	0.04136804	FASN/ EIF4EBP1	2

Table 2. CONTINUATION

Ontology	ID	Description	Gene Ratio	Bg Ratio	p	p adjust	q	geneID	Count
KEGG	hsa04910	Insulin signaling pathway	2/5	137/8164	0.00270445	0.05414617	0.04136804	FASN/ EIF4EBP1	2
KEGG	hsa04218	Cellular senescence	2/5	156/8164	0.0034933	0.05414617	0.04136804	TGFB1/ EIF4EBP1	2
KEGG	hsa05163	Human cytomegalovirus infection	2/5	225/8164	0.00715783	0.08875712	0.06781104	CXCR4/ EIF4EBP1	2

BP: biological process; CC: cellular component; MF: molecular function.

components (CC) such as platelet alpha granule and its subcompartments (membrane, lumen); molecular functions (MF) such as fatty acid synthase activity, TGF- $\beta$  receptor type I binding, and eukaryotic initiation factor 4E binding. KEGG pathway analysis revealed involvement in the intestinal immune network for IgA production, the insulin signaling pathway, and the AMP-activated protein kinase (AMPK) signaling pathway. Results were visualized as bar charts (Fig. 3A) and bubble plots (Fig. 3B), and functional networks were constructed for BP (Fig. 3C), MF (Fig. 3D), CC (Fig. 3E), and KEGG pathways (Fig. 3F).

Results of Gene Set Enrichment Analysis (GSEA)

GSEA of the GSE59034 dataset revealed significant associations between global gene expression patterns and key biological processes (Fig. 4A), including interleukin-10 signaling (Fig. 4B), neutrophil degranulation (Fig. 4C), Leishmania infection responses (Fig. 4D), and proinflammatory/profibrotic mediator networks (Fig. 4E). These findings, detailed in Table S2, demonstrate broad enrichment in immune-metabolic pathways, highlighting their potential role in obesity-related pathophysiology.

Differential expression and ROC analyses of A&GRDEGs

Wilcoxon rank-sum tests revealed significant differential expression ( $p < 0.05$ )

of three A&GRDEGs (*EIF4EBP1*, *TGFB1*, *SNCA*) between obese and control groups in the GSE134913 dataset (Fig. 5A). ROC analysis demonstrated strong diagnostic potential for *EIF4EBP1* (AUC = 0.921, Fig. 5D) and moderate predictive accuracy for *FASN* (AUC = 0.750), *SNCA* (AUC = 0.833), *TGFB1* (AUC = 0.798), and *CXCR4* (AUC = 0.762) (Fig. 5C-E), with AUC values indicating their utility as potential biomarkers for obesity classification.

Consistent analysis of the GSE59034 dataset revealed significant differential expression ( $p < 0.05$ ) for all five A&GRDEGs between obese and control groups (Fig. 5B). ROC analysis demonstrated excellent diagnostic performance for *EIF4EBP1* (AUC = 0.980) and *TGFB1* (AUC = 0.910), moderate accuracy for *FASN* (AUC = 0.828), and limited predictive value for *SNCA* (AUC = 0.699) and *CXCR4* (AUC = 0.691) (Fig. 5F-H).

Analysis of immune cell infiltration

Comparative analysis of immune cell infiltration using Wilcoxon rank-sum tests revealed significant abundance differences ( $p < 0.05$ ) for 26 of 28 immune cell types between obese and control groups in the GSE59034 dataset (Fig. 6A). Correlation analysis of these differentially abundant immune populations identified a particularly strong positive association ( $r = 0.98$ ) between activated dendritic cells and myeloid-derived suppressor cells (MDSCs) (Fig. 6B).



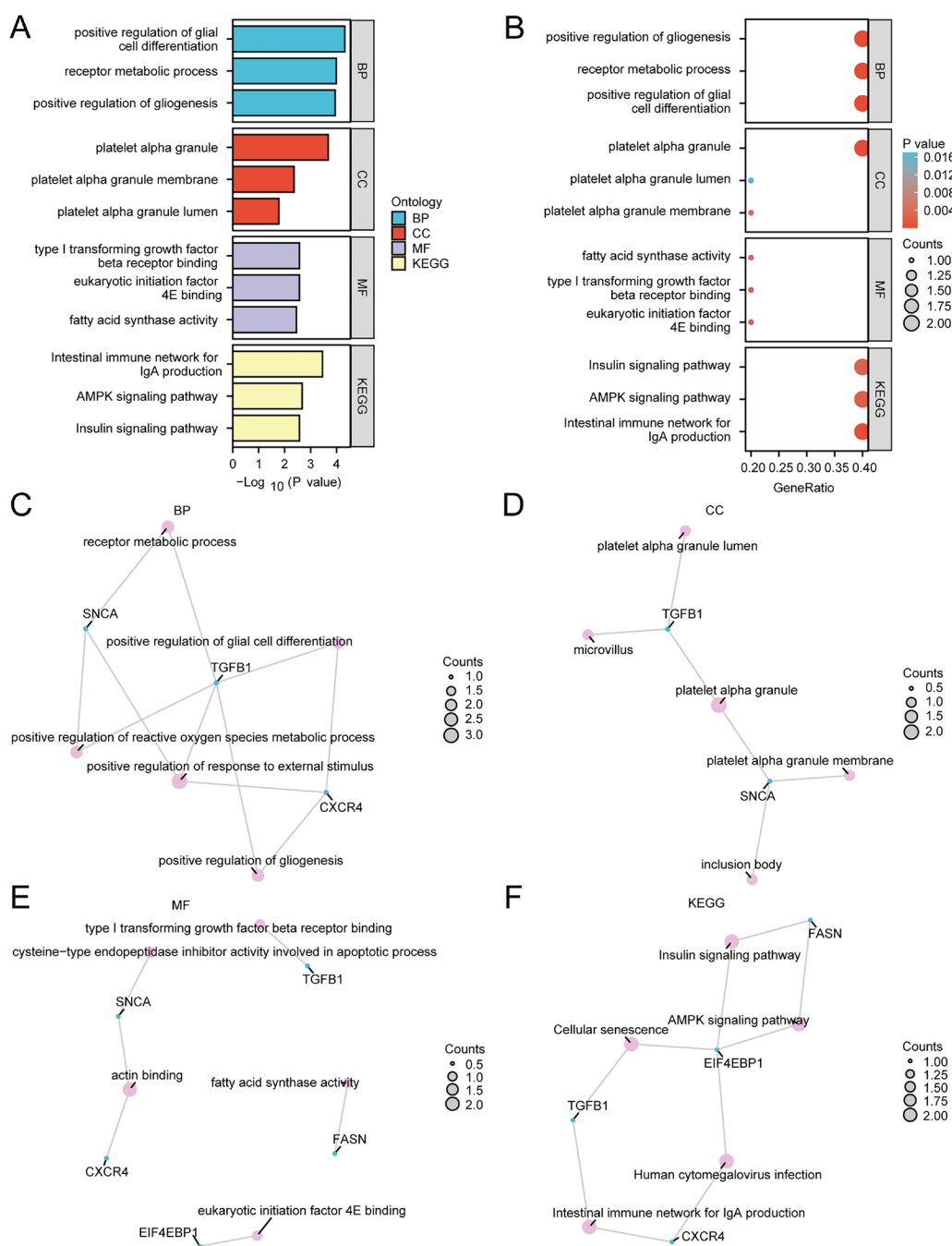


**Fig. 3.** GO and KEGG analyses.

(A) Bar charts of GO and KEGG analysis results for A&GRDEGs. The vertical axis shows GO and KEGG terms. (B) Bubble charts of GO and KEGG analysis results for A&GRDEGs. The vertical axis shows GO and KEGG terms. (C–E) Network diagrams of GO enrichment analysis for A&GRDEGs (C: BP, D: CC, E: MF). (F) Network diagrams of KEGG enrichment analysis for A&GRDEGs. In the network diagrams (C–F), pink dots represent specific pathways and blue dots represent specific genes. In the bubble charts, the bubble size represents the number of genes, and the bubble color represents the p-value, with redder hues indicating smaller values and bluer hues indicating larger values. The screening criteria for GO and KEGG analyses were  $p < 0.05$  and  $q < 0.25$ .

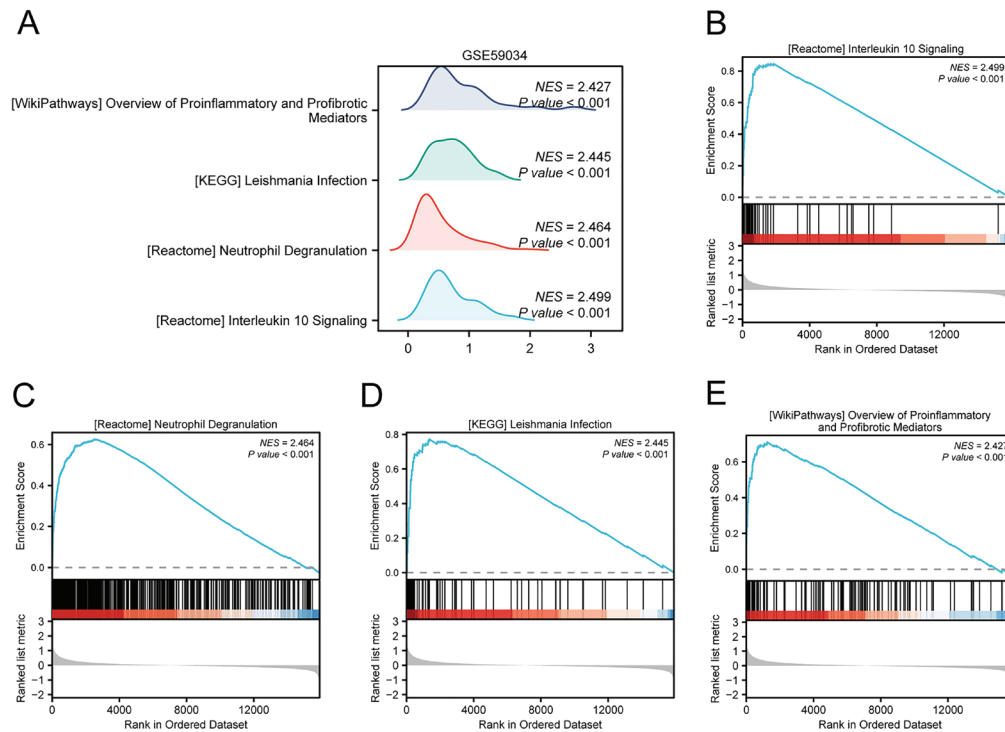


Fig. 4. GSEA of the GSE59034 dataset.

(A) Ridgeline plots of the four main biological functions in GSEA for the GSE59034 dataset. (B–E) Genes in the GSE59034 dataset were significantly enriched in interleukin 10 signaling (B), neutrophil degranulation (C), leishmania infection (D) and overview of proinflammatory and profibrotic mediators (E). The screening criteria for GSEA were  $p < 0.05$  and  $q < 0.25$ . NES, normalized enrichment score.

Correlation analysis between the 26 differentially abundant immune cell types and A&GRDEG expression levels in GSE59034 revealed a strong positive association between *TGFB1* expression and MDSC infiltration ( $r = 0.94$ ), and a significant negative correlation between *EIF4EBP1* levels and Th1 cell abundance ( $r = -0.87$ ) (Fig. 6C).

## DISCUSSION

The continuous rise of the obesity rate requires multifaceted and effective prevention and treatment. Inflammatory programs are activated during the early stages of adipose tissue expansion and during chronic obesity, thus perpetuating a proinflammatory phenotype in the immune system. This metabolic dysregulation may elevate the risk of developing severe comorbidities, includ-

ing insulin resistance, T2DM, cardiovascular disease, NAFLD, certain malignancies, and neurodegenerative disorders<sup>23</sup>. Inhibition of glycolysis has been shown to suppress macroautophagy and chaperone-mediated autophagy, leading to increased lipid accumulation<sup>24</sup>. The mechanisms of both autophagy and glycolysis in obesity-associated diseases are currently hot topics in research. Further research on the regulatory mechanisms of autophagy and the effects of glycolysis levels on obesity and chronic inflammation will help formulate more effective treatment strategies for obesity control.

By phosphorylating the EIF4EBP1, mTOR could dissociate from eIF4E and promote the initiation of translation<sup>25</sup>. Therefore, EIF4EBP1 is believed to be closely related to a wide range of diseases through its regulation of autophagy and glycolysis<sup>26,27</sup>.

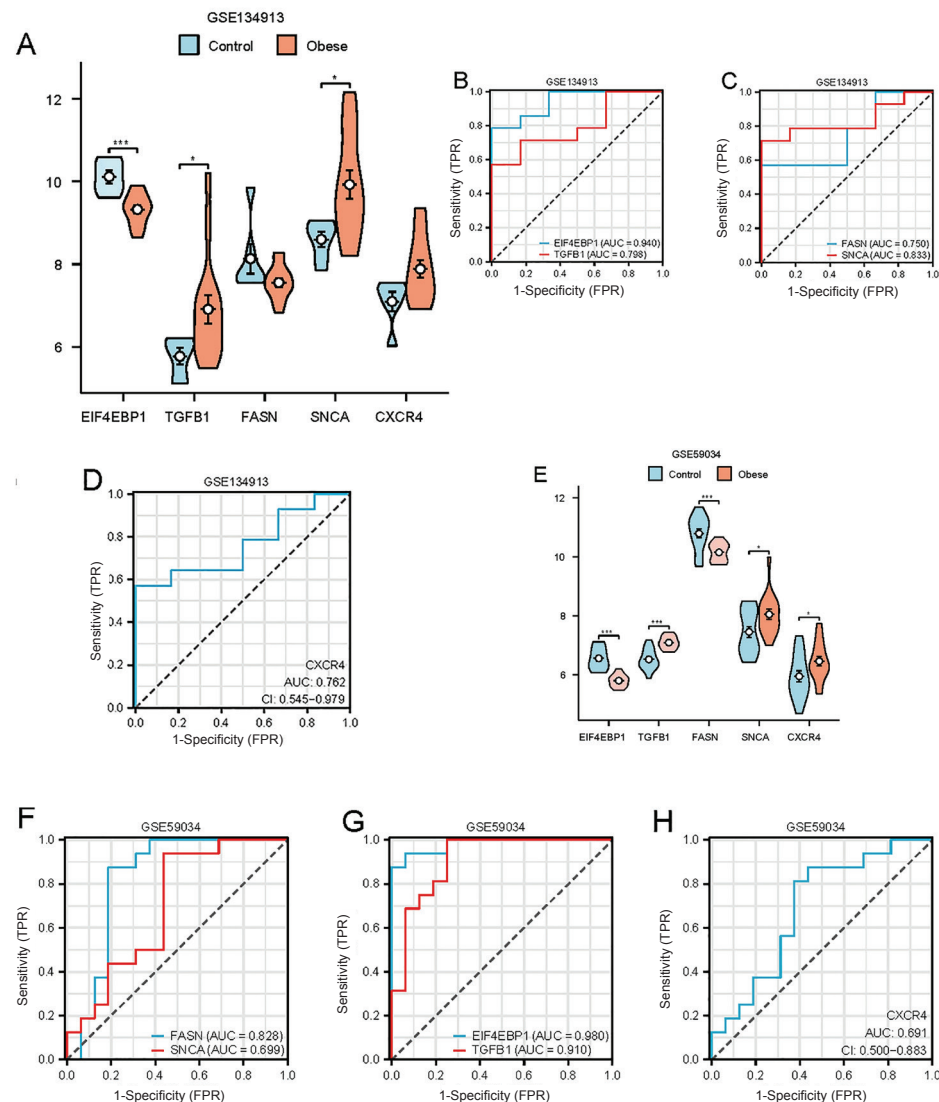


**Fig. 5.** Differential expression and ROC analyses of A&GRDEGs.

(A) Group comparison plot of A&GRDEGs between the obese and control groups in the GSE134913 dataset. (B) Group comparison plot of A&GRDEGs between the obese and control groups in the GSE59034 dataset. (C–E) ROC curves of A&GRDEGs: *FASN* and *SNCA* (C), *EIF4EBP1* and *TGFB1* (D), and *CXCR4* (E) between different groups (obese or control) in the GSE134913 dataset. (F–H) ROC curves of A&GRDEGs: *FASN* and *SNCA* (F), *EIF4EBP1* and *TGFB1* (G), and *CXCR4* (H) between different groups (obese or control) in the GSE59034 dataset. \* $p < 0.05$ ; \*\*\* $p < 0.001$ .

Experimental studies demonstrate that mTOR target proteins EIF4EBP1 and EIF4EBP2 play critical roles in metabolic regulation. Genetic ablation of both EIF4EBP1 and EIF4EBP2 exacerbates diet-induced obesity in murine models<sup>28</sup>. Conversely, enhanced EIF4EBP1 activity in skeletal muscle confers

metabolic protection, mitigating age- and diet-induced insulin resistance while maintaining energy expenditure. This protective effect is associated with reduced white adipose tissue accumulation and preserved brown adipose tissue mass<sup>29</sup>. The above results are consistent with the findings of this

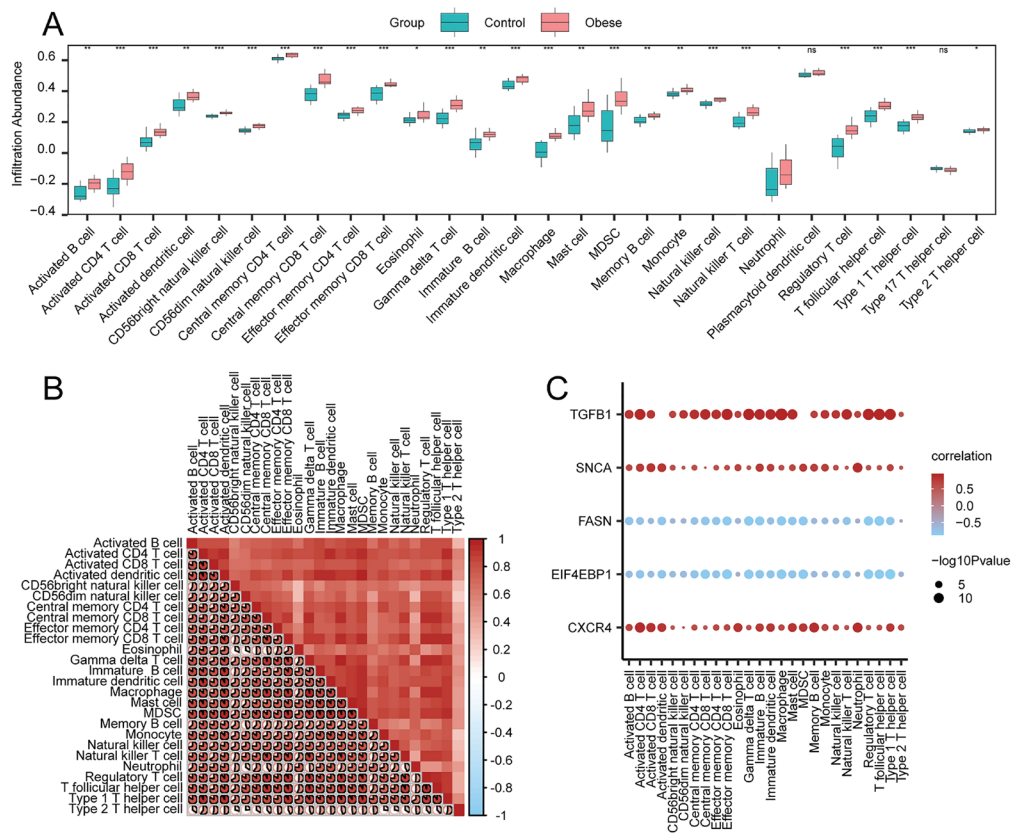


Fig. 6. ssGSEA of the GSE59034 dataset.

(A) Group comparison box plots of immune cells under the obese and control groups in the GSE59034 dataset. (B) Heatmap of correlations among the 26 immune cell types with significant differences in the GSE59034 dataset. (C) Correlation dot plot between the expression levels of A&GRDEGs and the abundance of 26 infiltrating immune cell types. Red indicates positive correlation and blue indicates negative correlation, with the shade of color indicating the strength of correlation. ns  $p \geq 0.05$ ; \*  $p < 0.05$ ; \*\*  $p < 0.01$ ; \*\*\*  $p < 0.001$ .

study, EIF4EBP1 is closely related to the regulatory mechanisms of obesity and chronic inflammation. However, the mechanisms by which EIF4EBP1 regulates obesity and chronic inflammation through autophagy and glycolysis require further study.

Patients with hyperlipidemia exhibit elevated levels of TGF- $\beta$ 1, which could suppress the function of natural killer (NK) cells, whereas restoring NK cell function could improve the prognosis of patients with metabolic syndrome<sup>30</sup>. Studies have shown that TGF- $\beta$ 1 could promote autophagy via the Smad and non-Smad pathways, driving hepatic fibrosis in NAFLD, and the progres-

sion of cardiac and renal fibrosis after ionizing radiation<sup>31,32</sup>. TGF- $\beta$ 1 induces metabolic reprogramming in target cells, shifting energy production from mitochondrial oxidative phosphorylation to glycolytic metabolism – a phenomenon consistent with the Warburg effect observed in many pathological states<sup>33</sup>. Systemic blocking of TGF- $\beta$ 1 signaling regulates glucose tolerance and energy homeostasis, protecting mice from obesity, diabetes, and fatty liver disease<sup>34</sup>. TGF- $\beta$ 1 directly modulates PBX-regulating protein-expression in both adipose-derived stem cells and mature adipocytes, thereby regulating adipogenic differentiation and insulin

sensitivity<sup>35</sup>. Many studies have shown a relationship between TGF- $\beta$ 1 and obesity and chronic inflammation, consistent with our study. However, there is no research on the mechanism of TGF- $\beta$ 1 inhibiting obesity and chronic inflammation by regulating autophagy and glycolysis levels, which is worthy of further exploration.

FASN is a key enzyme in hepatic de novo lipogenesis, while its upregulation is associated with insulin resistance<sup>36</sup>. Compared with normal-weight patients, FASN expression is significantly downregulated in patients with obesity<sup>37</sup>. Studies have demonstrated that the effect of hepatic FASN deficiency on NAFLD and diabetes is dependent on the etiology of obesity<sup>36</sup>. In mice with diet-induced obesity, adipose-specific FASN knockout aggravated high-fat diet-induced metabolic disturbances, exacerbating both hyperglycemia and hepatic dysfunction. These effects may be mediated through impaired hepatic glucose uptake secondary to glycogen accumulation and suppressed glycolytic flux<sup>36</sup>. The elevated FASN expression observed in obesity may confer a proliferative advantage to malignant cells through enhanced lipogenesis, potentially promoting tumorigenesis in obese microenvironments<sup>38</sup>. However, research has shown that renal cancer patients with obesity or overweight have a longer median overall survival owing to low FASN expression<sup>37</sup>. Therefore, considering the presence of obesity or overweight is important in future interventional treatments targeting the FASN pathway.

The high expression levels of the SNCA gene are closely associated with earlier onset, more rapid progression, and more severe manifestation of Parkinson's disease<sup>39</sup>. The SNCA gene encodes  $\alpha$ -synuclein. Mitochondrial accumulation of  $\alpha$ -synuclein aggregates triggers apoptotic pathways through multiple mechanisms, including mitochondrial permeability transition pore opening, calcium efflux, cytochrome C release, and subsequent mitochondrial swelling<sup>40</sup>. Importantly, high-fat diet-induced obesity

was shown to accelerate the onset of motor deficits in human  $\alpha$ -synuclein-expressing transgenic mice, correlating with premature  $\alpha$ -synucleinopathy development and astrogliosis<sup>41</sup>. These findings suggest that diet-induced metabolic dysfunction may represent a significant environmental risk factor for  $\alpha$ -synuclein pathology progression. Hence, molecular and cellular mechanisms underlying the interactions between obesity and SNCA in cognitive disorders await further elucidation.

CXCR4, the exclusive receptor for chemokine (C-X-C motif) ligand 12, orchestrates neutrophil metabolic reprogramming toward glycolysis and lactate production, while driving neutrophil accumulation in both circulation and psoriatic skin lesions<sup>42</sup>. Beyond its inflammatory functions, metabolic stress induces fat mass and obesity-related protein (FTO)-dependent N6-methyladenosine (m6A) mRNA demethylation, which upregulates CXCR4 expression via autophagic pathways. This mechanism critically contributes to melanoma pathogenesis and confers resistance to PD-1 checkpoint inhibition<sup>43</sup>. Moreover, inhibition of CXCR4 led to the sensitization of osteosarcoma to doxorubicin via the induction of autophagic cell death<sup>44</sup>. In summary, CXCR4 is closely related to inflammation, autophagy, and glycolysis, and hence its regulatory role in patients with obesity warrants further exploration.

Functional enrichment analysis revealed that the five A&GRDEGs were significantly associated with five key biological processes: insulin signaling, AMPK-mediated metabolic regulation, intestinal immune network for IgA production, cellular senescence pathways, and human cytomegalovirus (CMV) infection response. Among these, biological processes such as insulin resistance, AMPK signaling pathway, intestinal IgA immunity, and cellular senescence are thought to be closely related to chronic low-grade inflammation in patients with obesity<sup>45-48</sup>. GSEA of the GSE59034 dataset demonstrated significant enrichment of pro-inflammatory



and pro-fibrotic pathways in obesity. Notably, three metabolic regulators (*EIF4EBP1*, *FASN*, and *TGFBI*) exhibited consistent diagnostic accuracy across both datasets (Fig. 5). These findings implicate autophagy-glycolysis crosstalk in obesity pathogenesis, potentially through the amplification of inflammatory and fibrotic cascades. However, whether these five A&GRDEGs could be applied clinically for the prevention and treatment of obesity needs to be confirmed through further investigations.

Among the five A&GRDEGs, *TGFBI*, *SNCA*, and *CXCR4* expression positively correlated with immune cell recruitment, while *FASN* and *EIF4EBP1* showed significant inverse associations with immune infiltration levels. This dichotomous relationship suggests differential roles in immunometabolic regulation within obese adipose tissue. *TGFBI* showed the strongest positive correlation with MDSCs, while *EIF4EBP1* showed the strongest negative correlation with Th1 cells. Th1 cells, playing a facilitatory role in the pathogenesis of autoimmune diseases and tissue inflammatory responses, is regulated by cytokines IFN- $\gamma$ <sup>49</sup>. Furthermore, an elevated Th1 cell count was linked with elevated adipose tissue inflammation and insulin resistance, with its cell count increasing alongside increasing obesity<sup>50</sup>. *In vitro* evidence demonstrates that IFN- $\gamma$  exacerbates adipose tissue inflammation in obesity, while IFN- $\gamma$  knockout mice show improved metabolic profiles, including enhanced insulin sensitivity and reduced inflammatory markers in high-fat diet models<sup>51</sup>. However, the mechanistic relationship between *EIF4EBP1* expression and Th1 cell infiltration in obese adipose tissue remains unexplored. This knowledge gap highlights the need for focused investigations into *EIF4EBP1*-mediated immunometabolic regulation in chronic inflammation associated with obesity.

This study also has some limitations. First, the results from the two datasets included were not completely consistent, highlighting the need for experimental validation

and prospective clinical studies, which represent an important direction for our future research. Second, although screening was performed on obesity-related A&GRDEGs, the specific mechanisms of action involved were not clarified, which warrants further investigation.

In conclusion, levels of autophagy and glycolysis exhibit substantial predictive value for obesity development and mechanistically contribute to disease pathogenesis through immunometabolic dysregulation. These results provide a foundational framework for understanding obesity-associated chronic inflammation, offering new molecular targets for both basic research and potential therapeutic development.

### Acknowledgements

The authors gratefully acknowledge the data provided by patients and researchers participating in GEO.

### Funding

This research received no specific grant from any funding agency in the public, commercial, or not-for-profit sectors.

### Conflict of interests

All authors declare that they have no conflict of interest.

### Ethics approval and consent to participate

Not applicable, because GEO belongs to public databases, the patients involved in the database have obtained ethical approval, users can download relevant data for free for research and publish relevant articles, and our study is based on open-source data, and the The Fifth Affiliated Hospital of Sun Yat-sen University does not require research using publicly available data to be submitted for review to their ethics committee, so there are no ethical issues and other conflicts of interest.

### Consent for publication

Not applicable.

### Availability of data and materials

The original contributions presented in the study are included in the article/Supplementary material; further inquiries can be directed to the corresponding author.

### ORCID Numbers

- Simin Yang (SY):  
0009-0008-4837-9124
- Rexidanmu Hudabai (RH):  
0009-0005-8911-5916
- Xinwei Su (XS):  
0009-0001-4289-7018

### Authors' contributions

SY designed the research, collected the data, performed the statistical analysis, and drafted the manuscript. RH collected the data and performed the statistical analysis. XS supervised the statistical analysis, reviewed, and edited the manuscript. All authors have approved the final manuscript.

### REFERENCES

1. Ghaben AL, Scherer PE. Adipogenesis and metabolic health. *Nat Rev Mol Cell Biol.* 2019;20(4):242-258. <https://doi.org/10.1038/s41580-018-0093-z>.
2. Kim DS, Scherer PE. Obesity, Diabetes, and Increased Cancer Progression. *Diabetes Metab J.* 2021;45(6):799-812. <https://doi.org/10.4093/dmj.2021.0077>.
3. Calle EE, Kaaks R. Overweight, obesity and cancer: epidemiological evidence and proposed mechanisms. *Nat Rev Cancer.* 2004;4(8):579-591. <https://doi.org/10.1038/nrc1408>.
4. Namkoong S, Cho CS, Semple I, Lee JH. Autophagy Dysregulation and Obesity-Associated Pathologies. *Mol Cells.* 2018;41(1):3-10. <https://doi.org/10.14348/molcells.2018.2213>.
5. Tooze SA, Dikic I. Autophagy Captures the Nobel Prize. *Cell.* 2016;167(6):1433-1435. <https://doi.org/10.1016/j.cell.2016.11.023>.
6. Zhang Y, Sowers JR, Ren J. Targeting autophagy in obesity: from pathophysiology to management. *Nat Rev Endocrinol.* 2018;14(6):356-376. <https://doi.org/10.1038/s41574-018-0009-1>.
7. Dann SG, Selvaraj A, Thomas G. mTOR Complex1-S6K1 signaling: at the crossroads of obesity, diabetes and cancer. *Trends Mol Med.* 2007;13(6):252-259. <https://doi.org/10.1016/j.molmed.2007.04.002>.
8. Behrooz AB, Cordani M, Fiore A, Donadelli M, Gordon JW, Klionsky DJ, et al. The obesity-autophagy-cancer axis: Mechanistic insights and therapeutic perspectives. *Semin Cancer Biol.* 2024;99:24-44. <https://doi.org/10.1016/j.semcancer.2024.01.003>.
9. Soto-Herederó G, Gomez de Las Heras MM, Gabande-Rodríguez E, Oller J, Mittelbrunn M. Glycolysis - a key player in the inflammatory response. *FEBS J.* 2020;287(16):3350-3369. <https://doi.org/10.1111/febs.15327>.
10. Chang CH, Curtis JD, Maggi LB, Jr., Faubert B, Villarino AV, O'Sullivan D, et al. Posttranscriptional control of T cell effector function by aerobic glycolysis. *Cell.* 2013;153(6):1239-1251. <https://doi.org/10.1016/j.cell.2013.05.016>.
11. Jiao P, Chen Q, Shah S, Du J, Tao B, Tzamelis I, et al. Obesity-related upregulation of monocyte chemotactic factors in adipocytes: involvement of nuclear factor-kappaB and c-Jun NH2-terminal kinase pathways. *Diabetes.* 2009;58(1):104-115. <https://doi.org/10.2337/db07-1344>.
12. O'Rourke RW, White AE, Metcalf MD, Olivas AS, Mitra P, Larison WG, et al. Hypoxia-induced inflammatory cytokine secretion in human adipose tissue stromovascular cells. *Diabetologia.* 2011;54(6):1480-1490. <https://doi.org/10.1007/s00125-011-2103-y>.
13. Boutens L, Hooiveld GJ, Dhingra S, Cramer RA, Netea MG, Stienstra R. Unique metabolic activation of adipose

- tissue macrophages in obesity promotes inflammatory responses. *Diabetologia*. 2018;61(4):942-953. <https://doi.org/10.1007/s00125-017-4526-6>.
14. **Jacks RD, Lumeng CN.** Macrophage and T cell networks in adipose tissue. *Nat Rev Endocrinol*. 2024;20(1):50-61. <https://doi.org/10.1038/s41574-023-00908-2>.
  15. **Gancheva S, Ouni M, Jelenik T, Koliaki C, Szendroedi J, Toledo FGS, et al.** Dynamic changes of muscle insulin sensitivity after metabolic surgery. *Nat Commun*. 2019;10(1):4179. <https://doi.org/10.1038/s41467-019-12081-0>.
  16. **Petrus P, Mejhert N, Corrales P, Lecoutre S, Li Q, Maldonado E, et al.** Transforming Growth Factor- $\beta$ 3 Regulates Adipocyte Number in Subcutaneous White Adipose Tissue. *Cell Rep*. 2018;25(3):551-560.e5. <https://doi.org/10.1016/j.celrep.2018.09.069>.
  17. **Sun S, Shen Y, Wang J, Li J, Cao J, Zhang J.** Identification and Validation of Autophagy-Related Genes in Chronic Obstructive Pulmonary Disease. *Int J Chron Obstruct Pulmon Dis*. 2021;16:67-78. <https://doi.org/10.2147/copd.S288428>.
  18. **Fu D, Zhang B, Wu S, Zhang Y, Xie J, Ning W, et al.** Prognosis and Characterization of Immune Microenvironment in Acute Myeloid Leukemia Through Identification of an Autophagy-Related Signature. *Front Immunol*. 2021;12:695865. <https://doi.org/10.3389/fimmu.2021.695865>.
  19. **Wang N, Wei L, Liu D, Zhang Q, Xia X, Ding L, et al.** Identification and Validation of Autophagy-Related Genes in Diabetic Retinopathy. *Front Endocrinol (Lausanne)*. 2022;13:867600. <https://doi.org/10.3389/fendo.2022.867600>.
  20. **Zhang D, Zheng Y, Yang S, Li Y, Wang M, Yao J, et al.** Identification of a Novel Glycolysis-Related Gene Signature for Predicting Breast Cancer Survival. *Front Oncol*. 2020;10:596087. <https://doi.org/10.3389/fonc.2020.596087>.
  21. **Zheng J, Guo J, Zhu L, Zhou Y, Tong J.** Comprehensive analyses of glycolysis-related lncRNAs for ovarian cancer patients. *J Ovarian Res*. 2021;14(1):124. <https://doi.org/10.1186/s13048-021-00881-2>.
  22. **Bi J, Bi F, Pan X, Yang Q.** Establishment of a novel glycolysis-related prognostic gene signature for ovarian cancer and its relationships with immune infiltration of the tumor microenvironment. *J Transl Med*. 2021;19(1):382. <https://doi.org/10.1186/s12967-021-03057-0>.
  23. **Saltiel AR, Olefsky JM.** Inflammatory mechanisms linking obesity and metabolic disease. *J Clin Invest*. 2017;127(1):1-4. <https://doi.org/10.1172/JCI92035>.
  24. **Zhang T, Linghu KG, Tan J, Wang M, Chen D, Shen Y, et al.** TIGAR exacerbates obesity by triggering LRRK2-mediated defects in macroautophagy and chaperone-mediated autophagy in adipocytes. *Autophagy*. 2024;20(8):1741-1761. <https://doi.org/10.1080/15548627.2024.2338576>.
  25. **Bjornsti MA, Houghton PJ.** Lost in translation: dysregulation of cap-dependent translation and cancer. *Cancer Cell*. 2004;5(6):519-523. <https://doi.org/10.1016/j.ccr.2004.05.027>.
  26. **Chen C, Chen W, Nong Z, Nie Y, Chen X, Pan X, et al.** Hyperbaric oxygen alleviated cognitive impairments in mice induced by repeated cerebral ischemia-reperfusion injury via inhibition of autophagy. *Life Sci*. 2020;241:117170. <https://doi.org/10.1016/j.lfs.2019.117170>.
  27. **Selvarajah B, Azuelos I, Plate M, Guillion D, Forty EJ, Contento G, et al.** mTORC1 amplifies the ATF4-dependent de novo serine-glycine pathway to supply glycine during TGF- $\beta$ (1)-induced collagen biosynthesis. *Sci Signal*. 2019;12(582):eaav3048. <https://doi.org/10.1126/scisignal.aav3048>.
  28. **Le Bacquer O, Petroulakis E, Paglialunga S, Poulin F, Richard D, Cianflone K, et al.** Elevated sensitivity to diet-induced obesity and insulin resistance in mice lacking 4E-BP1 and 4E-BP2. *J Clin Invest*. 2007;117(2):387-396. <https://doi.org/10.1172/JCI29528>.
  29. **Tsai S, Sitzmann JM, Dastidar SG, Rodriguez AA, Vu SL, McDonald CE, et al.** Muscle-specific 4E-BP1 signaling activation improves metabolic parameters

- during aging and obesity. *J Clin Invest*. 2015;125(8):2952-2964. <https://doi.org/10.1172/JCI77361>.
30. Hu X, Jia X, Xu C, Wei Y, Wang Z, Liu G, et al. Downregulation of NK cell activities in Apolipoprotein C-III-induced hyperlipidemia resulting from lipid-induced metabolic reprogramming and crosstalk with lipid-laden dendritic cells. *Metabolism*. 2021;120:154800. <https://doi.org/10.1016/j.metabol.2021.154800>.
  31. Siapoush S, Rezaei R, Alavifard H, Hatami B, Zali MR, Vosough M, et al. Therapeutic implications of targeting autophagy and TGF-beta crosstalk for the treatment of liver fibrosis. *Life Sci*. 2023;329:121894. <https://doi.org/10.1016/j.lfs.2023.121894>.
  32. Ahamed J, Laurence J. Role of Platelet-Derived Transforming Growth Factor-beta1 and Reactive Oxygen Species in Radiation-Induced Organ Fibrosis. *Antioxid Redox Signal*. 2017;27(13):977-988. <https://doi.org/10.1089/ars.2017.7064>.
  33. Hewitson TD, Smith ER. A Metabolic Reprogramming of Glycolysis and Glutamine Metabolism Is a Requisite for Renal Fibrogenesis-Why and How? *Front Physiol*. 2021;12:645857. <https://doi.org/10.3389/fphys.2021.645857>.
  34. Yadav H, Quijano C, Kamaraju AK, Gavrilova O, Malek R, Chen W, et al. Protection from obesity and diabetes by blockade of TGF-beta/Smad3 signaling. *Cell Metab*. 2011;14(1):67-79. <https://doi.org/10.1016/j.cmet.2011.04.013>.
  35. Bruno A, Di Sano C, Simon HU, Chanez P, Patti AM, Di Vincenzo S, et al. Leptin and TGF-beta1 Downregulate PREP1 Expression in Human Adipose-Derived Mesenchymal Stem Cells and Mature Adipocytes. *Front Cell Dev Biol*. 2021;9:700481. <https://doi.org/10.3389/fcell.2021.700481>.
  36. Matsukawa T, Yagi T, Uchida T, Sakai M, Mitsushima M, Naganuma T, et al. Hepatic FASN deficiency differentially affects nonalcoholic fatty liver disease and diabetes in mouse obesity models. *JCI Insight*. 2023;8(17):e161282. <https://doi.org/10.1172/jci.insight.161282>.
  37. Albiges L, Hakimi AA, Xie W, McKay RR, Simantov R, Lin X, et al. Body Mass Index and Metastatic Renal Cell Carcinoma: Clinical and Biological Correlations. *J Clin Oncol*. 2016;34(30):3655-3663. <https://doi.org/10.1200/JCO.2016.66.7311>.
  38. Khandekar MJ, Cohen P, Spiegelman BM. Molecular mechanisms of cancer development in obesity. *Nat Rev Cancer*. 2011;11(12):886-895. <https://doi.org/10.1038/nrc3174>.
  39. Ross OA, Braithwaite AT, Skipper LM, Kachergus J, Hulihan MM, Middleton FA, et al. Genomic investigation of alpha-synuclein multiplication and parkinsonism. *Ann Neurol*. 2008;63(6):743-750. <https://doi.org/10.1002/ana.21380>.
  40. Malpartida AB, Williamson M, Narendra DP, Wade-Martins R, Ryan BJ. Mitochondrial Dysfunction and Mitophagy in Parkinson's Disease: From Mechanism to Therapy. *Trends Biochem Sci*. 2021;46(4):329-343. <https://doi.org/10.1016/j.tibs.2020.11.007>.
  41. Rotermund C, Truckenmuller FM, Schell H, Kahle PJ. Diet-induced obesity accelerates the onset of terminal phenotypes in alpha-synuclein transgenic mice. *J Neurochem*. 2014;131(6):848-858. <https://doi.org/10.1111/jnc.12813>.
  42. Chen J, Bai Y, Xue K, Li Z, Zhu Z, Li Q, et al. CREB1-driven CXCR4(hi) neutrophils promote skin inflammation in mouse models and human patients. *Nat Commun*. 2023;14(1):5894. <https://doi.org/10.1038/s41467-023-41484-3>.
  43. Yang S, Wei J, Cui YH, Park G, Shah P, Deng Y, et al. m(6)A mRNA demethylase FTO regulates melanoma tumorigenicity and response to anti-PD-1 blockade. *Nat Commun*. 2019;10(1):2782. <https://doi.org/10.1038/s41467-019-10669-0>.
  44. Liao YX, Lv JY, Zhou ZF, Xu TY, Yang D, Gao QM, et al. CXCR4 blockade sensitizes osteosarcoma to doxorubicin by inducing autophagic cell death via PI3K-Akt-mTOR pathway inhibition. *Int J Oncol*. 2021;59(1):49. <https://doi.org/10.3892/ijo.2021.5229>.
  45. Esser N, LeGrand-Poels S, Piette J, Scheen AJ, Paquot N. Inflammation as a

- link between obesity, metabolic syndrome and type 2 diabetes. *Diabetes Res Clin Pract.* 2014;105(2):141-150. <https://doi.org/10.1016/j.diabres.2014.04.006>.
46. **Foretz M, Guigas B, Viollet B.** Understanding the glucoregulatory mechanisms of metformin in type 2 diabetes mellitus. *Nat Rev Endocrinol.* 2019;15(10):569-589. <https://doi.org/10.1038/s41574-019-0242-2>.
47. **Huus KE, Petersen C, Finlay BB.** Diversity and dynamism of IgA-microbiota interactions. *Nat Rev Immunol.* 2021;21(8):514-525. <https://doi.org/10.1038/s41577-021-00506-1>.
48. **Ferrucci L, Fabbri E.** Inflammageing: chronic inflammation in ageing, cardiovascular disease, and frailty. *Nat Rev Cardiol.* 2018;15(9):505-522. <https://doi.org/10.1038/s41569-018-0064-2>.
49. **Huh JY, Park YJ, Ham M, Kim JB.** Crosstalk between adipocytes and immune cells in adipose tissue inflammation and metabolic dysregulation in obesity. *Mol Cells.* 2014;37(5):365-371. <https://doi.org/10.14348/molcells.2014.0074>.
50. **Schipper HS, Prakken B, Kalkhoven E, Boes M.** Adipose tissue-resident immune cells: key players in immunometabolism. *Trends Endocrinol Metab.* 2012;23(8):407-415. <https://doi.org/10.1016/j.tem.2012.05.011>.
51. **Rocha VZ, Folco EJ, Sukhova G, Shimizu K, Gotsman I, Vernon AH, et al.** Interferon- $\gamma$ , a Th1 cytokine, regulates fat inflammation: a role for adaptive immunity in obesity. *Circ Res.* 2008;103(5):467-476. <https://doi.org/10.1161/CIRCRESA-HA.108.177105>.